Radiation pattern shaping of a mobile base station antenna array using a particle swarm optimization based technique

Article *in* Electrical Engineering · April 2008

DOI: 10.1007/s00202-007-0078-y

CITATIONS
13

READS
3,888

1 author:

Zaharias D. Zaharis
Aristotle University of Thessaloniki
166 PUBLICATIONS **1,353** CITATIONS

SEE PROFILE

Electr Eng (2008) 90:301–311
DOI 10.1007/s00202-007-0078-y

ORIGINAL PAPER

Radiation pattern shaping of a mobile base station antenna array using a particle swarm optimization based technique

Z. D. Zaharis

Received: 18 July 2006 / Accepted: 9 June 2007 / Published online: 18 July 2007

Abstract A new technique of shaping the radiation pattern of an antenna array is presented. The technique aims at finding the appropriate geometry of the antenna array as well as the excitation of the array elements in order to produce a radiation pattern of the desired shape. A suitable optimization procedure is applied using a particle swarm optimization algorithm. The technique has been successfully applied to collinear arrays and seems to be suitable for beam-forming of antenna arrays used by mobile communications base stations.

Keywords Radiation pattern shaping · Antenna array synthesis · Antenna beam-forming · Base station antennas · Particle swarm optimization

1 Introduction

The present mobile communications systems organize the service area into geographically separated areas, known as cells. Each cell is served by a base station that represents the interface to the fixed network. Frequency reuse strategy is the basis of cellular systems [1–4]. A reuse pattern is established using clusters of N cells and each one of these N cells uses a different frequency. Every cluster of cells uses the same set of frequencies according to the reuse pattern. In this way, cells that use the same frequency are far enough and thus the interference between these cells is kept at a tolerable level. Consequently, the frequency reuse allows modern systems to provide much higher capacity than older systems where the available frequency channels were used only once to cover a large metropolitan area. A reuse pattern using clusters of three cells with corresponding frequencies f_1, f_2, f_3 is illustrated in Fig. 1. The service area is a cell covered by a base station operating at frequency f_1. The same frequency is used by another cell far enough from the previous one. Potentially the two cells could interfere with each other. The interference depends on many parameters and one of them is the behavior of the transmitting antenna used by the base station. The behavior is described by means of the far-field radiation pattern of the antenna on the vertical plane. In particular, two basic requirements must be satisfied regarding the radiation pattern in order to reduce the interference. First, the main lobe of the pattern must tilt down from the horizontal plane so as to distribute its radiation power only inside the service area, which is determined in the spherical coordinate system by the negative vertical direction $\theta = 180°$ and the direction $\theta = \theta_B$ (as shown in Fig. 1). According to the second requirement, the antenna gain $G(\theta)$ between the directions $\theta = 0$ and $\theta = \theta_A$ must be low enough compared to the maximum gain G_{max} of the main lobe. Of course, the low $G(\theta)$ is crucial not only to reduce the interference but also to minimize the power loss caused by spatial spread of radiated power. It must be noted that the power spread between $\theta = 0$ and $\theta = \theta_A$ may be not only due to side lobes of the radiation pattern but due to a part of the main lobe as well. The second requirement is considered to be satisfied if the $G(\theta)$ between $\theta = 0$ and $\theta = \theta_A$ is equal to or less than -20 dB with respect to G_{max}. This condition is defined by the expression

$$10 \log \frac{G(\theta)}{G_{max}} \leq -20\,\text{dB}, \quad 0 \leq \theta \leq \theta_A \tag{1}$$

or by the equivalent form

$$\frac{G(\theta)}{G_{max}} \leq \frac{1}{100}, \quad 0 \leq \theta \leq \theta_A \tag{2}$$

Z. D. Zaharis (✉)
Department of Electronics, Technological Educational Institute of Thessaloniki, Sindos, 57400 Thessaloniki, Greece
e-mail: zaharis@auth.gr

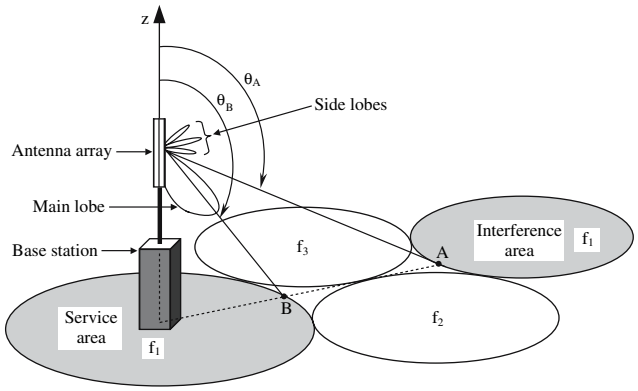

Fig. 1 Cellular mobile communications structure

Another major issue is how the main lobe distributes the power inside the service area. In this case, the power P_R received by a mobile station is required to be the same regardless of the position of the mobile station inside the cell. Considering free space environment (Fig. 2), P_R is given by the Friis transmission equation [5]:

$$P_R = P_T\, G_T(\theta)\, G_R(\theta) \left(\frac{\lambda}{2\pi\, r}\right)^2 \tag{3}$$

where P_T is the power transmitted by the base station antenna, λ is the wavelength, r is the distance between the antennas of the base station and the mobile station, and finally $G_T(\theta)$ and $G_R(\theta)$ are the gains of the two respective antennas along the direction of the distance r, which is determined by the elevation angle θ. Using the geometry of Fig. 2, Eq. (3) takes

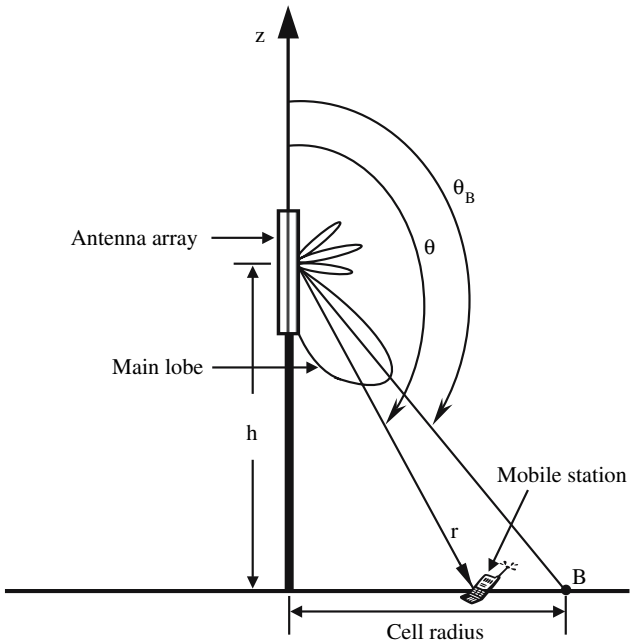

Fig. 2 Main lobe shaping inside the service area

the following form:

$$P_R = P_T\, G_T(\theta)\, G_R(\theta) \left(\frac{\lambda}{2\pi\, h}\right)^2 \cos^2\theta \tag{4}$$

where h is the antenna height (in meters) above local ground level. G_R is considered constant because in practice it does not change notably with angle θ. Then, for a given P_T and under the requirement of constant P_R mentioned above, Eq. (4) yields

$$G_T(\theta) = \frac{P_R}{P_T\, G_R(\theta)} \left(\frac{2\pi\, h}{\lambda}\right)^2 \sec^2\theta \tag{5}$$

which means that the main radiation lobe of the base station antenna must distribute the power inside the service area according to the term $\sec^2\theta$.

In conclusion, the desired radiation pattern of a base station antenna must satisfy two conditions: (a) $G_T(\theta) \leq G_{Tmax}/100$ between $\theta = 0$ and $\theta = \theta_A$, and (b) the main lobe must distribute the power inside the service area determined by $\theta = \theta_B$ and $\theta = 180°$ according to the term $\sec^2\theta$ ($G_T(\theta) \sim \sec^2\theta$). We may refer to the above two conditions, respectively, as "condition for low interference" and "condition for optimum main lobe shaping". The sector of the radiation pattern between $\theta = \theta_A$ and $\theta = \theta_B$ is of no interest because it corresponds to cells where the frequency of operation is different than f_1 (see Fig. 1) and thus there is no chance of interference with these cells.

In addition, a well-designed antenna must satisfy the "impedance-matching condition", meaning that the input impedance Z_{in} of the antenna has to be as close as possible to the characteristic impedance Z_o of the feeding line. The impedance-matching condition is described in terms of the standing wave ratio (SWR) at the input of the antenna. The optimum value of SWR is 1 and is reached when $Z_{in} = Z_o$, but this hardly ever happens. The impedance-matching condition is considered to be satisfied when the SWR is below 2 (SWR < 2). According to the transmission line theory [6,7] the complex reflection coefficient at the input of the antenna is given by

$$R = \frac{Z_{in} - Z_o}{Z_{in} + Z_o} \tag{6}$$

where Z_o is considered equal to 50 Ohm. Thus, the SWR is calculated by the following expression:

$$\text{SWR} = \frac{1 + |R|}{1 - |R|} \tag{7}$$

where $|R|$ is the amplitude of R.

In the recent past, a lot of work has been performed on various types of pattern shaping, depending each time on the requirements of the specific application [8–15]. The present study describes a new method of radiation pattern shaping that can be implemented in practice. The method has been

applied to collinear antenna arrays composed of wire dipoles. The arrays are analyzed by using the Method of Moments [5,16–18]. Realistic effects are taken into account such as the mutual coupling between the dipoles. The antenna arrays are considered to be used by mobile communications base stations. So, their radiation pattern must be shaped according to the conditions for low interference and for optimum main lobe shaping. In addition, the arrays must satisfy the impedance-matching condition and therefore SWR < 2 for each array element. In order to achieve these conditions, an optimization procedure is performed using a particle swarm optimization (PSO) algorithm [19–32] developed by the author. The basic idea implemented by the PSO algorithm is the maximization of a particular mathematical function called "fitness function". The fitness function is suitably determined according to the above three conditions. When these conditions are satisfied, the fitness function finds its global maximum value and the algorithm terminates with success.

2 Particle swarm optimization

The concept of function optimization by means of a particle swarm was introduced in [19]. The method is based on the intelligence and movement of swarms. In nature, the swarm intelligence is the main attribute that helps the swarm to find the place where there is more food than anywhere else. A good example to understand the swarm intelligence is the behavior of a swarm of bees. The intension of the bees is to find the location with the highest density of flowers. Each bee makes random movements with random velocities looking for flowers. The bee has the ability to remember the position where it found the most flowers and is aware in someway of the positions where the other bees found plenty of flowers. During flight, each bee adjusts its position according to its own experience, and according to the experience of the neighboring bees. In fact, the bee takes into account the best positions encountered by itself and by its neighbors. So, its movement is an attempt to balance exploration and exploitation. Finally, this behavior leads the bees to the one point with the highest density of flowers. Unable to find any other place where the flower concentration is even higher, the bees go back to this point. The modeling of the above behavior results in the PSO method.

In PSO terminology [19–32], every individual in the swarm is called "particle" or "agent". The number S of the particles that compose the swarm is called "population size". The experience indicates that a population size between 10 and 50 is optimal for many problems (e.g., $S = 30$). All the particles act in the same way like bees do, i.e., they move in the search space and update their velocity according to the best positions already found by themselves and by their neighbors, trying to find an even better position. Each particle is treated as point in an N-dimensional space. The position of the i-th particle ($i = 1, \ldots, S$) is represented as $\vec{x}_i = (x_{i1}, x_{i2}, \ldots, x_{i\mathrm{N}})$, where x_{in} ($n = 1, \ldots, N$) are the position coordinates. Each coordinate x_{in} may be limited in the respective (n-th) dimension between an upper boundary U_n and a lower boundary L_n, so that $L_n \leq x_{in} \leq U_n$ ($n = 1, \ldots, N$). The difference $R_n = U_n - L_n$ between the two boundaries is called "dynamic range" of the n-th dimension. The performance of each particle is measured according to a predefined mathematical function F called "fitness function", which is related to the problem to be solved. The value of the fitness function depends on the position coordinates, i.e., $F = F(\vec{x}_i) = F(x_{i1}, x_{i2}, \ldots, x_{i\mathrm{N}})$. Actually, the particle position is considered to be improved as the value of the fitness function is increased. The best previous position (pbest position) of the i-th particle is recorded and represented as $\vec{p}_i = (p_{i1}, p_{i2}, \ldots, p_{i\mathrm{N}})$. The change of $\vec{x}_i$ is $\Delta\vec{x}_i = \vec{v}_i\,\Delta t$, where Δt is the time interval, $\vec{v}_i = (v_{i1}, v_{i2}, \ldots, v_{i\mathrm{N}})$ is the velocity of the i-th particle and v_{in} ($n = 1, \ldots, N$) are the velocity coordinates. The calculation of the velocity is explained below. Considering that $\Delta t = 1$, the position change becomes $\Delta\vec{x}_i = \vec{v}_i$. Thus, the new position of the i-th particle after a time step is given by

$$\vec{x}_i(t+1) = \vec{x}_i(t) + \vec{v}_i(t+1) \tag{8}$$

Particle swarms have been studied in two types of neighborhood, called "gbest" and "lbest". In the gbest neighborhood, every particle is attracted to the best position found by any particle of the swarm. This position, called "gbest position", is represented as $\vec{g} = (g_1, g_2, \ldots, g_N)$ and corresponds to the maximum fitness value $F_{\max} = F(\vec{g}) = F(g_1, g_2, \ldots, g_N)$ found so far by the swarm. The gbest neighborhood is equivalent to a fully connected social network. Every individual is able to compare the performances of every other member of the population, imitating the very best. In the lbest neighborhood, each (i-th) individual is affected by the best performance of its K_i immediate neighbors, i.e., the i-th individual is attracted to the best position found by its K_i neighbors. This position, called "lbest position", is represented as $\vec{\ell}_i = (\ell_{i1}, \ell_{i2}, \ldots, \ell_{i\mathrm{N}})$ and corresponds to the maximum value $F_{\max,i} = F(\vec{\ell}_i) = F(\ell_{i1}, \ell_{i2}, \ldots, \ell_{i\mathrm{N}})$ of the fitness function found so far by the K_i neighbors of the i-th particle. These K_i neighbors are not necessarily particles who are near the individual in the parameter space, but rather ones that are near it in a topological space. The optimal pattern of connectivity among individuals depends on the problem being solved. The lore suggests that using the gbest neighborhood the swarm tends to converge more rapidly on optima (when it is going to converge), but it is more susceptible to convergence on local optima.

As mentioned above, individuals are influenced by their own previous behavior and by the successes of their neighbors. So, the particle's velocity depends on its previous velocity, on the distance between the particle's position and the best position found by the particle so far and finally on the distance between the particle's position and the best position found so far by the swarm (for gbest model) or by the particle's neighborhood (for lbest model). According to the gbest model, the velocity of the i-th particle after a time step is given by

$$\vec{v}_i(t+1) = w\,\vec{v}_i(t) + c_1\,\text{rand}\,(t)\left[\vec{p}_i(t) - \vec{x}_i\,(t)\right] + c_2\,\text{rand}(t)\left[\vec{g}(t) - \vec{x}_i(t)\right] \tag{9}$$

where w is a positive parameter called "inertia weight", c_1 and c_2 are positive parameters called respectively "cognitive coefficient" and "social coefficient", and rand(t) is a function that generates random numbers drawn from a uniform distribution between 0.0 and 1.0. According to the lbest model, the only change is to substitute $\vec{\ell}_i$ for $\vec{g}$. Thus, Eq. (9) is modified as follows:

$$\vec{v}_i(t+1) = w\,\vec{v}_i(t) + c_1\,\text{rand}(t)\left[\vec{p}_i(t) - \vec{x}_i(t)\right] + c_2\,\text{rand}(t)\left[\vec{\ell}_i(t) - \vec{x}_i(t)\right] \tag{10}$$

The weight w usually has fixed values between 0.0 and 1.0, and controls the impact of the previous values of velocity on the current velocity value. A larger w facilitates global exploration, while a smaller w tends to facilitate local exploration to fine-tune the current search area. Suitable choices of w provide a balance between global and local exploration abilities and thus require fewer iterations to find the optimum [20]. A good approach is to decrease w linearly from 0.9 to 0.4 during the course of a simulation [21]. The same value of w is used for all dimensions of all particles in a given population. The coefficient c_1 determines how much the particle is influenced by the memory of its best location, while c_2 determines how much the particle is influenced by the swarm (for gbest model) or by its neighbors (for lbest model). It was suggested [22] that the best choice for both c_1 and c_2 is 2.0.

It is easy to realize that the changes in the velocity are stochastic and an undesirable effect is that the particle's trajectory can expand into wider and wider cycles through the problem space, eventually approaching infinity. One method of solving the problem is to implement a maximum allowed velocity $\vec{v}_{\max} = \left(v_{\max,1}, v_{\max,2}, \ldots, v_{\max,N}\right)$. So, for each ($i$-th) particle and each ($n$-th) dimension, if $v_{in} > v_{\max,n}$ then $v_{in} = v_{\max,n}$, and also if $v_{in} < -v_{\max,n}$ then $v_{in} = -v_{\max,n}$. $\vec{v}_{\max}$ has the beneficial effect of preventing explosion and scales the exploration of the particle's search. Unfortunately, the choice of a value for $\vec{v}_{\max}$ depends on the problem. For example, the particle will be trapped if a step larger than $\vec{v}_{\max}$ is required to escape a local optimum. However, in approaching an optimum it is better to take smaller steps. It was found [22] that if $w = 1$ it is better to set each coordinate $v_{\max,n}$ around 10–20% of the dynamic range R_{n} of the respective dimension, and if $w < 1$ it is better to set $v_{\max,n} = R_n$ ($n = 1, \ldots, N$).

A recent analysis of the PSO [23] presents an alternative way of calculation of the velocity. According to the gbest model, the velocity of the i-th particle after a time step is calculated by

$$\vec{v}_i(t+1) = k\left\{\vec{v}_i(t) + \varphi_1\text{rand}(t)\left[\vec{p}_i(t) - \vec{x}_i(t)\right] + \varphi_2\text{rand}(t)\left[\vec{g}(t) - \vec{x}_i(t)\right]\right\} \tag{11}$$

while, according to the lbest model, the velocity is given by

$$\vec{v}_i(t+1) = k\left\{\vec{v}_i(t) + \varphi_1\text{rand}(t)\left[\vec{p}_i(t) - \vec{x}_i(t)\right] + \varphi_2\text{rand}(t)\left[\vec{\ell}_i\,(t) - \vec{x}_i(t)\right]\right\} \tag{12}$$

In the above equations, the parameter k is called "constriction coefficient" and is defined by the following expression:

$$k = \frac{2}{\left|2 - \varphi - \sqrt{\varphi^2 - 4\varphi}\right|} \tag{13}$$

where the parameter φ, sometimes called "acceleration constant", must be greater than 4 ($\varphi > 4$) and is calculated by the expression:

$$\varphi = \varphi_1 + \varphi_2 \tag{14}$$

where the parameters φ_1 and φ_2 have the same meaning like c_1 and c_2, respectively. A standard choice recommended in [22] for both φ_1 and φ_2 is 2.05. The use of the constriction coefficient was another attempt to eliminate the need for $\vec{v}_{\max}$, but most authors agree that it is still better to use $\vec{v}_{\max}$ in order to keep the particles in bounds.

Nevertheless, the above parameters w, k, and $\vec{v}_{\max}$ are not always able to confine the particles within the search space, so that $L_n \le x_{in} \le U_n$ ($n = 1, \ldots, N$). To solve this problem, three different boundary conditions have been suggested: (a) The absorbing walls: when a particle hits U_n or L_n, v_{in} becomes zero and the particle is pulled back toward the search space, i.e., if $x_{in} > U_n$ then $x_{in} = U_n$ and $v_{in} = 0$, and also if $x_{in} < L_n$ then $x_{in} = L_n$ and $v_{in} = 0$. In that manner, the energy of the particles that try to escape the search space is considered to be absorbed by the boundary walls. (b) The reflecting walls: when a particle hits U_n or L_n, v_{in} is reversed (becomes $-v_{in}$) and the particle is reflected back toward the search space. (c) Invisible walls: the particles are allowed to move inside or outside the search space without any restriction, but the fitness function is not evaluated for those particles being outside the search space. Actually, this technique saves computational time because the fitness function is calculated only for the particles inside the search space.

3 Formulation

Using the theory described above, a PSO algorithm was developed by the author in order to shape the radiation patterns produced by wire-dipole antenna arrays and to match the array elements (i.e., the wire dipoles) to the feeding network. The lengths and the positions of the dipoles as well as the amplitude and phase of the excitation currents applied on the dipoles are considered as the position coordinates x_{in} of the particles. Given the values of x_{in} $(n = 1, \ldots, N)$, a corresponding value of the fitness function $F(x_{i1}, x_{i2}, \ldots, x_{iN})$ is derived for the position of the i-th particle. The structure of the fitness function is discussed below. The algorithm aims at finding the gbest coordinates g_n that correspond to the maximum fitness value $F_{\max}$. Actually, the g_n $(n = 1, \ldots, N)$ produce both the specific geometry and the specific excitation of the antenna array that achieve the desired shaping of the radiation pattern and match the array elements to the feeding network.

A swarm size of 30 particles ($S = 30$) is used in the algorithm. The velocity is calculated by Eq. (12) according to the lbest model, where each particle is affected by three neighbors ($K_i = 3$, for $i = 1, \ldots, S$). The parameters φ_1 and φ_2 are chosen equal to 2.05, and thus $\varphi = 4.10$. Then, Eq. (13) yields $k = 0.73$. Finally, the values of k, φ_1 and φ_2 are used in Eq. (12). The algorithm makes use of $\vec{v}_{\max}$, where $v_{\max,n} = 0.20R_n$ $(n = 1, \ldots, N)$. Also, the absorbing walls condition is used in order to confine the particles within the search space.

The structure of the PSO algorithm is given below:

1. Initialization.
   - (a) Initialize counters t (for time steps), n (for dimensions), and i (to count particles).
   - (b) Set random number seed.
   - (c) Set the values of N, S, K_i, φ_1, φ_2, $t_{\max}$ (total number of iterations) and the values of L_n, U_n, $v_{max,n}$ for $n = 1, \ldots, N$.
   - (d) Randomly initialize the particle positions $\vec{x}_i$ $(i = 1, \ldots, S)$ inside the search space, so that $L_n \leq x_{in} \leq U_n$ $(n = 1, \ldots, N)$.
   - (e) Randomly initialize the particle velocities $\vec{v}_i$ $(i = 1, \ldots, S)$. If $v_{in} > v_{\max,n}$ then $v_{in} = v_{\max,n}$, and also if $v_{in} < -v_{\max,n}$ then $v_{in} = -v_{\max,n}$.
   - (f) Evaluate the values of the fitness function $F(\vec{x}_i)$ $(i = 1, \ldots, S)$ for all the particles.
   - (g) Set $\vec{p}_i = \vec{x}_i$ and $F(\vec{p}_i) = F(\vec{x}_i)$ for $i = 1, \ldots, S$ (the first position of each particle is considered as pbest position).
   - (h) Find the maximum value $F_{\max}$ among the $F(\vec{p}_i)$ $(i = 1, \ldots, S)$. The position that corresponds to $F_{\max}$ is the gbest position $\vec{g}$, so that $F_{\max} = F(\vec{g})$.
2. Optimization.
   - (a) For each (i-th) particle, find randomly K_i particles, which are the neighbors of the i-th particle.
   - (b) Find the individual that gives the maximum fitness value $F_{\max,i}$ among the K_i neighbors of each (i-th) particle. The position of this individual is the lbest position $\vec{\ell}_i$ in the neighborhood of the i-th particle, so that $F_{\max,i} = F\left(\vec{\ell}_i\right)$.
   - (c) Update the particle velocities $\vec{v}_i$ $(i = 1, \ldots, S)$ using Eq. (12). If $v_{in} > v_{\max,n}$ then $v_{in} = v_{\max,n}$, and also if $v_{in} < -v_{\max,n}$ then $v_{in} = -v_{\max,n}$.
   - (d) Update the particle positions $\vec{x}_i$ $(i = 1, \ldots, S)$ using Eq. (8), and apply the absorbing walls condition.
   - (e) Evaluate the fitness value $F(\vec{x}_i)$ $(i = 1, \ldots, S)$ for all the particles.
   - (f) For each (i-th) particle, if $F(\vec{x}_i) > F(\vec{p}_i)$ $(i = 1, \ldots, S)$ then $\vec{p}_i = \vec{x}_i$ (the new position becomes pbest position of the i-th particle).
   - (g) For each (i-th) particle, if $F(\vec{p}_i) > F(\vec{g})$ $(i = 1, \ldots, S)$ then $\vec{g} = \vec{p}_i$ (the pbest position with the maximum fitness value in the swarm becomes gbest position).
   - (h) Increase the counter t by 1.
   - (i) If $t < t_{\max}$ and $F(\vec{g})$ was improved then go to 2(b). If $t < t_{\max}$ and $F(\vec{g})$ was not improved then go to 2(a) (meaning that the lbest neighborhood must be reinitialized for each particle).
3. Report results and terminate.

The PSO algorithm was applied on the antenna array of Fig. 3. The array consists of M collinear wire dipoles oriented in the vertical direction. All the dipoles are assumed to have the same radius of 0.001λ, where λ is the wavelength that corresponds to the operation frequency of the antenna array. Due to the orientation of the dipoles, the radiation pattern is omni-directional on the horizontal plane and thus the antenna array can be used by a mobile communications base station located at the center of a cell (i.e., a service area). The radiation pattern on the vertical plane depends on the geometry of the array as well as on the excitation currents applied in the middle of the length of the dipoles. The geometry of the array is specified by the lengths L_m $(m = 1, \ldots, M)$ of the dipoles and their positions z_m $(m = 2, \ldots, M)$ with respect to the position of the first dipole which is considered fixed at the origin of the coordinate system ($z_1 = 0$). Each excitation current is complex and therefore is specified by its amplitude I_m and its phase a_m. Given the values of the parameters mentioned above (i.e., L_m, z_m, I_m, and a_m), the antenna array is modeled as a wire grid and is analyzed by applying the method of moments (MoM) [5,16–18].

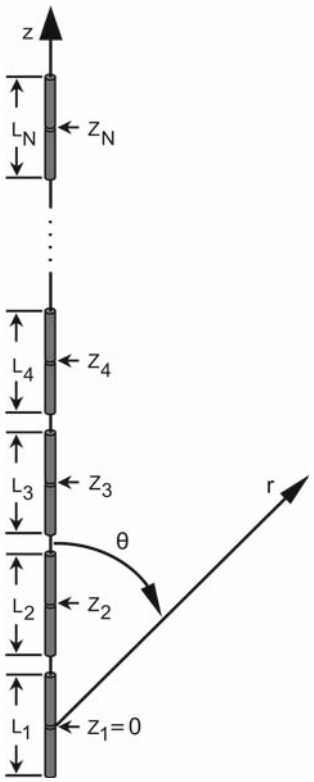

Fig. 3 Collinear wire dipole antenna array

The results derived from the MoM and used by the PSO algorithm is the variation of the antenna array gain $G(\theta)$, and the input impedances at the feeding points of the dipoles. In fact, $G(\theta)$ determines the far-field radiation pattern on the vertical plane, which is subject to shaping by the PSO algorithm according to the conditions for optimum main lobe shaping and for low interference. The condition for optimum main lobe shaping implies that inside the service area determined by $\theta = \theta_B$ and $\theta = 180°$, $G_d(\theta) \sim \sec^2\theta$ where $G_d(\theta)$ is the desired gain. For convenience, $G_d(\theta)$ is normalized with respect to its maximum value $G_{d,max}$ obtained for $\theta = \theta_B(G_{d,max} = G_d(\theta_B))$. Thus, the normalized desired gain is given by

$$G_{d,norm}(\theta) = \frac{G_d(\theta)}{G_d(\theta_B)} = \frac{\sec^2\theta}{\sec^2\theta_B}, \quad \theta_B \le \theta \le 180° \tag{15}$$

or, in decibels (dB), by the equivalent form

$$G^{dB}_{d,norm}(\theta) = 10\log\frac{G_d(\theta)}{G_d(\theta_B)} = 20\log\frac{\sec\theta}{\sec\theta_B}, \quad \theta_B \le \theta \le 180° \tag{16}$$

In a similar way, $G(\theta)$ can be normalized with respect to its maximum value G_{max}, which must be obtained for $\theta = \theta_B(G_{max} = G(\theta_B))$. Then, the normalized gain is given by

$$G_{norm}(\theta) = \frac{G(\theta)}{G(\theta_B)}, \quad 0^o \le \theta \le 180° \tag{17}$$

or, in dB, by the equivalent form

$$G^{dB}_{norm}(\theta) = 10\log\frac{G(\theta)}{G(\theta_B)}, \quad 0^o \le \theta \le 180° \tag{18}$$

The condition for low interference implies $G(\theta) \le G_{max}/100$ between $\theta = 0$ and $\theta = \theta_A$. Given that $G_{max} = G(\theta_B)$ and using Eq. (17), this condition can be expressed as follows:

$$G_{norm}(\theta) \le 10^{-2}, \quad 0 \le \theta \le \theta_A \tag{19}$$

or, in dB, by the equivalent expression

$$G^{dB}_{norm}(\theta) \le -20, \quad 0 \le \theta \le \theta_A \tag{20}$$

In addition, each dipole of the array must satisfy the impedance-matching condition (SWR $<$ 2). Equations (6) and (7) can be used for the calculation of SWR of the dipoles in the form given below:

$$R_m = \frac{Z_{in,m} - Z_o}{Z_{in,m} + Z_o}, \quad (m = 1, \ldots, M) \tag{21}$$

$$SWR_m = \frac{1 + |R_m|}{1 - |R_m|}, \quad (m = 1, \ldots, M) \tag{22}$$

where $Z_{in,m}$ and R_m are, respectively, the impedance and the complex reflection coefficient at the input of the m-th dipole, and $|R_m|$ is the amplitude of R_m.

In order to optimize the antenna array taking into account the three above conditions, it is necessary to construct a suitable fitness function. Therefore, the fitness function is formed as a weighted sum of three terms, where each term is constructed according to the respective condition. The first term F_1 corresponds to the condition for optimum main lobe shaping and is described by the following formula:

$$F_1 = \sum_{j=0}^{(180°-\theta_B)/\theta_S} \left|G_{norm}(\theta_B + j\theta_S) - G_{d,norm}(\theta_B + j\theta_S)\right| \tag{23}$$

θ_S is the increment step of θ and is determined externally (e.g., $\theta_S = 0.5°$). While the integer j counts from 0 to $(180° - \theta_B)/\theta_S$, the angle θ varies from θ_B to 180°. Actually, F_1 is a positive term that describes how much the radiation pattern deviates from its desired shape inside the service area. Normally, the integral

$$F_1 = \int_{\theta_B}^{180°} \left|G_{norm}(\theta) - G_{d,norm}(\theta)\right| \cdot d\theta \tag{24}$$

should be used for the calculation of F_1 but it needs much more computational time than Eq. (23). The second term

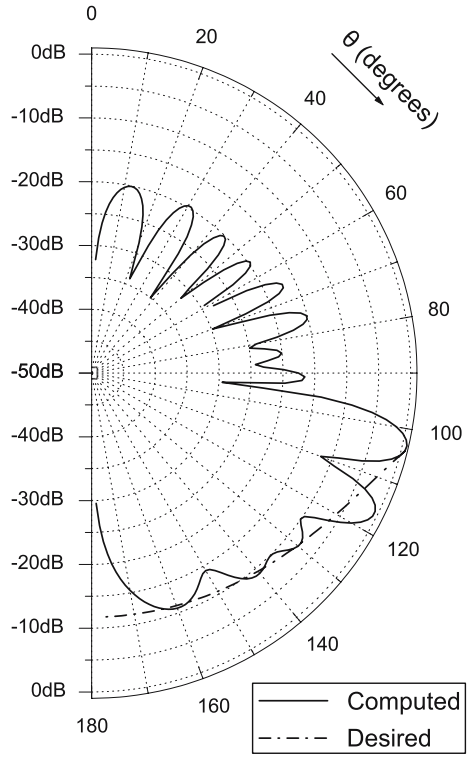

Fig. 4 Radiation pattern of an optimized collinear antenna array composed of ten wire dipoles that have the same fixed length, the same fixed excitation amplitude, and variable excitation phases. Required interference area: 0°–95°. Required service area: 105°–180°

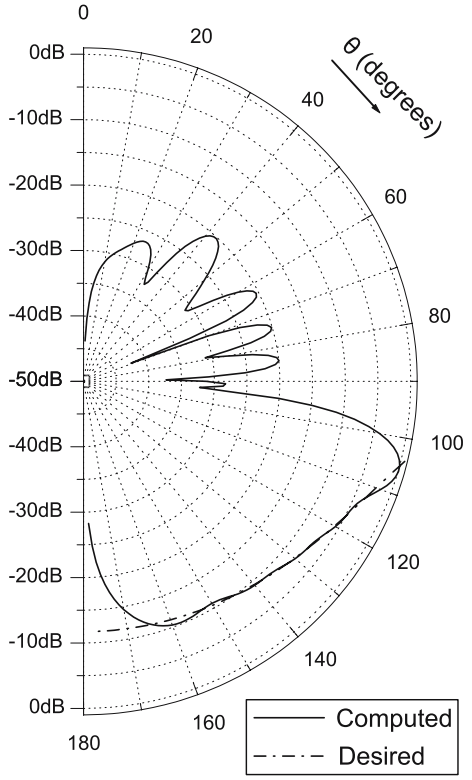

Fig. 5 Radiation pattern of an optimized collinear antenna array composed of ten wire dipoles that have the same variable length, variable excitation amplitudes, and variable excitation phases. Required interference area: 0°–95°. Required service area: 105°–180°

F_2 corresponds to the condition for low interference and is described by the formula

$$F_2 = \sum_{j=0}^{\theta_A/\theta_S} \left| g(j\theta_S) - 10^{-2} \right| \tag{25}$$

where

$$g(j\theta_S) = \begin{cases} G_{\text{norm}}(j\theta_S), & \text{if } G_{\text{norm}}(j\theta_S) > 10^{-2} \\ 10^{-2} & \text{if } G_{\text{norm}}(j\theta_S) \le 10^{-2} \end{cases} \tag{26}$$

While the integer j counts from 0 to θ_A/θ_S, the angle θ varies from 0 to θ_A. The meaning of Eq. (26) is that only values of G_{norm} greater than 10^{-2} affect F_2, because they do not satisfy the condition for low interference. The third term F_3 corresponds to the impedance-matching condition and is described by the formula

$$F_3 = \sum_{m=1}^{M} (\text{SWR}_m - 1) \tag{27}$$

F_3 has positive values and vanishes only when the optimum value of SWR is reached by all the dipoles. Finally, for any values of L_m, z_m, I_m, and a_m, the fitness function is evaluated by the expression

$$F(L_1, \ldots, L_M, z_2, \ldots, z_M, I_1, \ldots, I_M, a_1, \ldots, a_M) = W_1 \cdot F_1 + W_2 \cdot F_2 + W_3 \cdot F_3 \tag{28}$$

The coefficients W_1, W_2, and W_3 are weight factors and they declare the importance of the corresponding terms that compose the fitness function. Provided that the weight factors have negative values, F increases from negative values to zero, as the three above conditions tend to be satisfied. When F finds its global maximum value $F_{\max} = 0$, all the requirements are satisfied and the PSO algorithm terminates successfully.

4 Results

Several cases are studied in order to raise the performance of the PSO based technique. The first dipole (located at $z_1 = 0$) is considered as reference dipole. Thus, the excitation amplitude and phase of the rest dipoles are presented, respectively, with reference to the excitation amplitude and phase of the first dipole ($I_1 = 1, a_1 = 0$).

The optimization is initially focused on satisfying the conditions for optimum main lobe shaping and for low

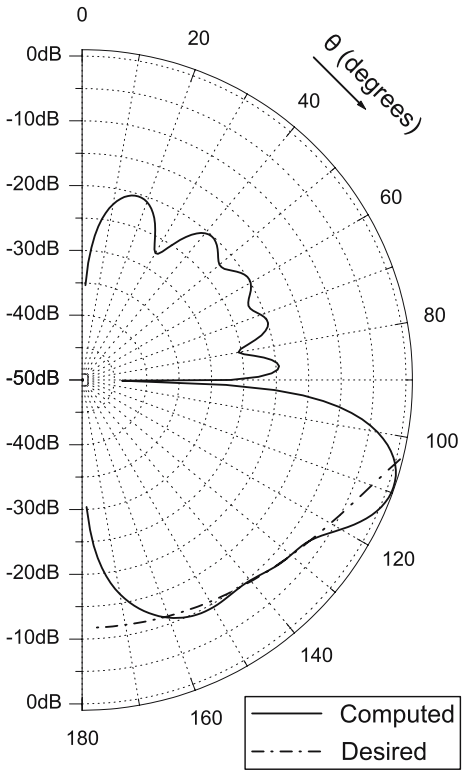

Fig. 6 Radiation pattern of an optimized collinear antenna array composed of six wire dipoles that have the same variable length, variable excitation amplitudes, and variable excitation phases. Required interference area: 0°–95°. Required service area: 105°–180°

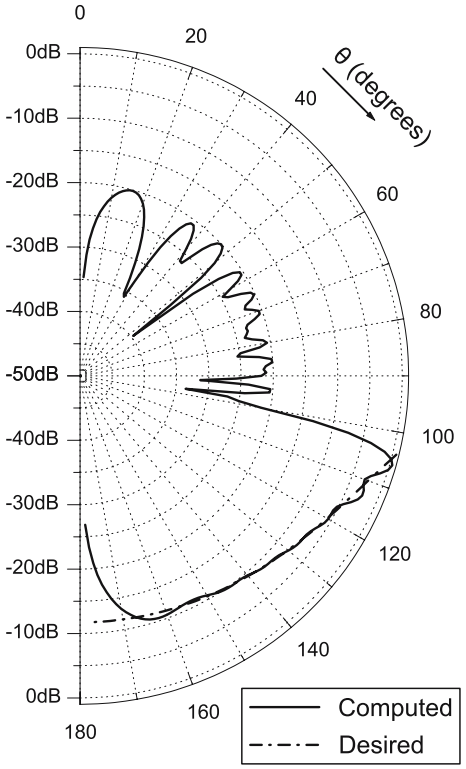

Fig. 7 Radiation pattern of an optimized collinear antenna array composed of 20 wire dipoles that have the same variable length, variable excitation amplitudes, and variable excitation phases. Required interference area: 0°–95°. Required service area: 105°–180°

interference. Thus, the impedance-matching condition is not taken into account and this is done by setting $W_3 = 0$ in Eq. (28). The required interference area is defined between $\theta = 0°$ and $\theta = 95°$, while the required service area is defined between $\theta = 105°$ and $\theta = 180°$. The angular width of 10° between the above areas is of no interest as explained in the introduction section of the paper. The antenna array consists of ten wire dipoles ($M = 10$) that all have the same radius of 0.001λ and the same length $L_m = 0.478\lambda$, $m = 1, \ldots, M$, which is the resonant length of a wire dipole with radius of 0.001λ in free space. The resonant length was found by analyzing a wire dipole in free space using the MoM. The positions z_m ($m = 2, \ldots, M$) of the dipoles are variable, while the excitation currents have the same fixed amplitude $I_m = 1, m = 1, \ldots, M$, and variable phases a_m. Phase variation is necessary because equal phases produce a broadside radiation pattern where the main lobe does not tilt down from the horizontal plane. This first effort to optimize the antenna array reveals many problems in the behavior of the array. The radiation pattern (Fig. 4) has side lobes in the interference area where the normalized gain is greater than −20 dB. Also, the pattern deviates notably from its desired shape inside the service area. In addition, the resulting values of SWR, which vary from 1.41 to 5.90, show that the dipoles are not in resonant condition. This happens due to mutual coupling between the dipoles and thus the impedance-matching condition is not satisfied, but as mentioned above this condition is not taken into account yet.

In order to approximate the desired radiation pattern, more variable parameters are needed. Therefore, the ten dipoles of the above antenna array have variable positions and the same length, but this time the length is variable. Moreover, the excitation currents have not only variable phases but also variable amplitudes. The optimization is performed in order to improve the radiation pattern (and not the SWR). The resulting pattern presented in Fig. 5 exhibits an excellent improvement. Not only is the normalized gain less than −20 dB in the interference area, but also the radiation pattern hardly deviates from its desired shape in the major part of the service area. The only remarkable deviation is noticed close to the negative vertical direction ($\theta = 180°$). This deviation is inevitable and it will be observed in all cases, because wire dipoles do not radiate along their axis in the far field.

It is very interesting to see how much the number of dipoles affects the radiation pattern. Optimizing the antenna array as given in the second case but composed of six dipoles ($M = 6$), we get the radiation pattern of Fig. 6 where the degradation of the pattern shape is obvious. On the contrary, if the

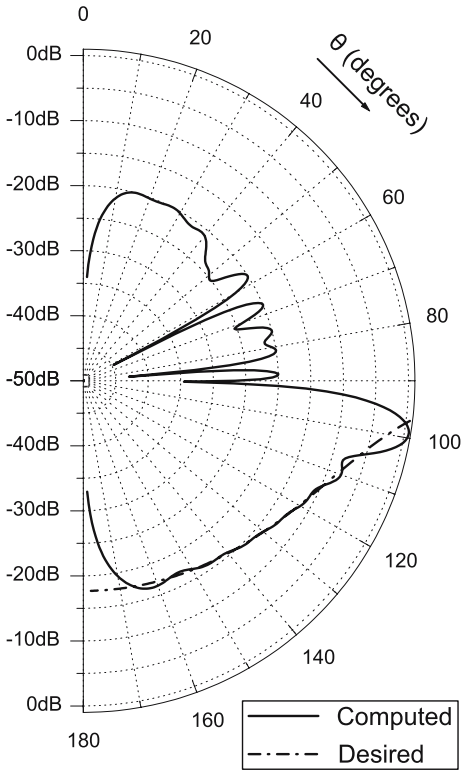

Fig. 8 Radiation pattern of an optimized collinear antenna array composed of ten wire dipoles that have the same variable length, variable excitation amplitudes, and variable excitation phases. Required interference area: 0°–92.5°. Required service area: 97.5°–180°

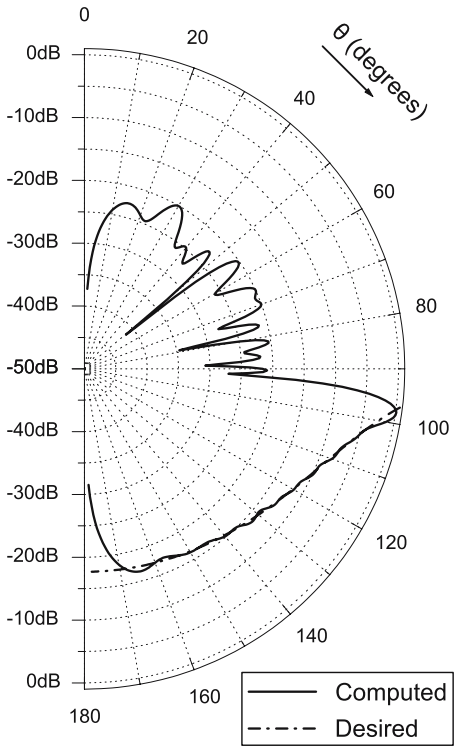

Fig. 9 Radiation pattern of an optimized collinear antenna array composed of 20 wire dipoles that have the same variable length, variable excitation amplitudes, and variable excitation phases. Required interference area: 0°–92.5°. Required service area: 97.5°–180°

antenna array consists of 20 dipoles ($M = 20$), the radiation pattern (Fig. 7) maintains its shape close to the desired one. The comparison between Figs. 5 and 7 shows that increasing the number of dipoles above ten does not improve significantly the radiation pattern. Therefore, using more dipoles than ten is not recommended because the computational time is unnecessarily increased.

In order to exhibit the performance of the technique, the requirements become more stringent. Thus, the angular width between the interference area and the service area is reduced to 5°, assuming that the radius of the cells (of the cellular communications system) is increased. The interference area is defined between $\theta = 0°$ and $\theta = 92.5°$, while the service area is defined between $\theta = 97.5°$ and $\theta = 180°$. The antenna array consists of ten dipoles that have variable positions and variable length, but the length is the same for all the dipoles. The excitation currents have variable amplitudes and variable phases. The optimization is performed in order to improve the radiation pattern (and not the SWR). The resulting pattern (Fig. 8) deviates notably from its desired shape inside the service area, and also the normalized gain is greater than -20 dB in directions close to $\theta_A = 92.5°$ inside the interference area. In this case, an increase in the number of dipoles is very helpful for the optimization process. It was found that if the antenna array given above consists of 20 dipoles, the radiation pattern is remarkably improved as shown in Fig. 9. However, using more dipoles than 20 is not recommended because the computational time is unnecessarily increased without improving significantly the radiation pattern.

So far, it has been shown that the PSO based technique is capable of finding structures that satisfy the conditions for optimum main lobe shaping and for low interference. In the cases given below, it will be shown that the impedance-matching condition can be satisfied for all the dipoles of the antenna array as well. In order to help the PSO algorithm find the optimal solution, more variable parameters are needed. Therefore, the ten dipoles of the above antenna array have variable lengths, which are different from each other. The excitation currents have variable phases and variable amplitudes, like the above cases. Initially, the interference area is defined between $\theta = 0°$ and $\theta = 95°$, while the service area is defined between $\theta = 105°$ and $\theta = 180°$. The resulting values of SWR vary from 1.0 to 1.4, and thus all the dipoles satisfy the impedance-matching condition. Moreover, the radiation pattern (Fig. 10) of the optimized structure

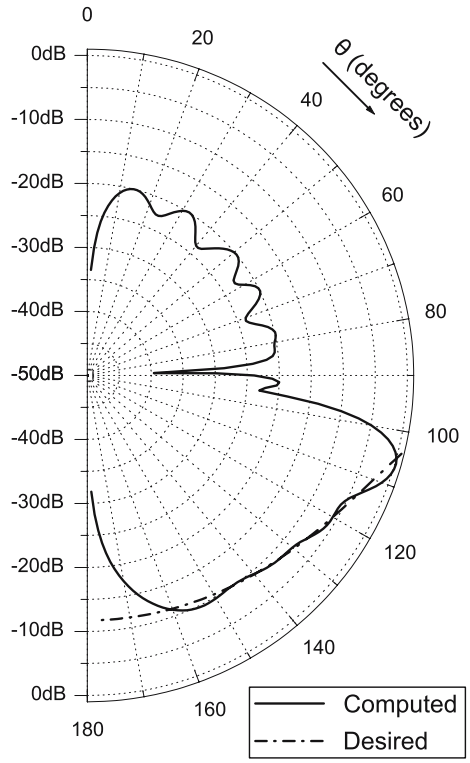

Fig. 10 Radiation pattern of an optimized collinear antenna array composed of ten wire dipoles that have variable lengths different from each other, variable excitation amplitudes, and variable excitation phases. Required interference area: 0°–95°. Required service area: 105°–180°. Resulting SWR_m ($m = 1, \ldots, 10$): 1.0, 1.3, 1.0, 1.0, 1.1, 1.4, 1.0, 1.2, 1.0, 1.0

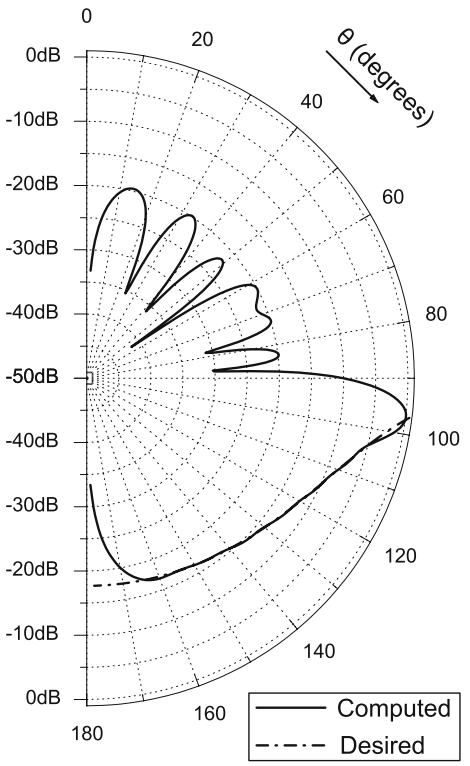

Fig. 11 Radiation pattern of an optimized collinear antenna array composed of ten wire dipoles that have variable lengths different from each other, variable excitation amplitudes, and variable excitation phases. Required interference area: 0°–92.5°. Required service area: 97.5°–180°. Resulting SWR_m ($m = 1, \ldots, 10$): 1.3, 1.3, 1.0, 1.2, 1.0, 1.6, 1.3, 1.3, 1.0, 1.0

meets the shaping requirements. The requirements become more demanding by defining, once again, the interference area between $\theta = 0°$ and $\theta = 92.5°$, and the service area between $\theta = 97.5°$ and $\theta = 180°$. The PSO algorithm optimizes the same 10-dipole array as given above. The resulting values of SWR vary from 1.0 to 1.6. Therefore, the optimization process is capable of finding a structure where all the dipoles are matched to the feeding network. Also, the radiation pattern presented in Fig. 11 is close to its desired shape inside the service area. However, the normalized gain is greater than −20 dB in directions close to $\theta_A = 92.5°$ inside the interference area, and thus the condition for low interference is not satisfied. As mentioned above, the only solution to the problem is an increase in the number of dipoles. So, if the antenna array given above consists of 20 dipoles, the radiation pattern is remarkably improved as shown in Fig. 12, because it satisfies both the conditions for optimum main lobe shaping and for low interference. In addition, the resulting values of SWR vary from 1.0 to 1.8, and thus the impedance-matching condition is also satisfied by all the dipoles of the array. It seems that there is always an optimal number of dipoles that makes the antenna array satisfy all the above conditions. This number is increased as the angular width between the interference area and the service area is reduced.

5 Conclusions

The cases studied in the present work show that the PSO based technique is capable of finding structures that satisfy the conditions for optimum main lobe shaping, for low interference and for impedance matching. The radiation patterns produced by the optimization procedure have the desired shape inside the service area, while the normalized antenna array gain is less than −20 dB inside the interference area. In addition, all the elements of the antenna array are matched to the feeding network. The ability to find structures that satisfy the impedance-matching condition makes the technique very useful in practice. It was also shown that the proposed technique is very promising even in cases where the requirements become more demanding. The antenna arrays derived from the above study have been optimized for mobile communications. But this is not the only usage of the optimization method. The proposed technique is suitable for optimizing

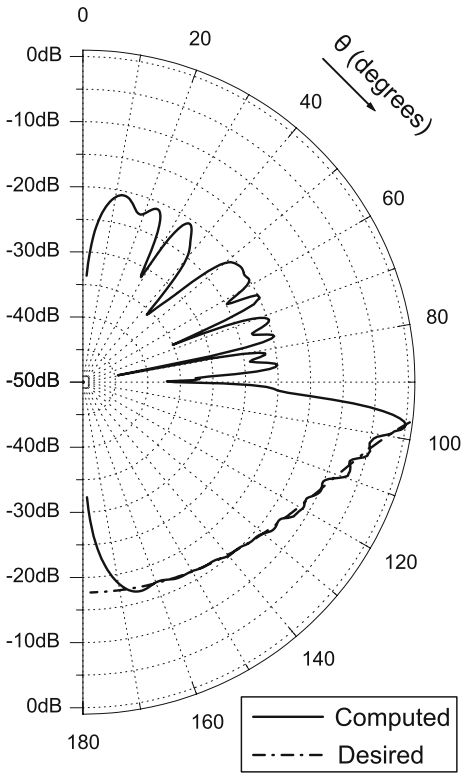

Fig. 12 Radiation pattern of an optimized collinear antenna array composed of 20 wire dipoles that have variable lengths different from each other, variable excitation amplitudes, and variable excitation phases. Required interference area: 0°–92.5°. Required service area: 97.5°–180°. Resulting SWR_m ($m = 1, \ldots, 20$): 1.3, 1.0, 1.4, 1.0, 1.8, 1.0, 1.7, 1.0, 1.4, 1.0, 1.4, 1.2, 1.2, 1.0, 1.7, 1.7, 1.4, 1.3, 1.2, 1.2

many types of antennas and thus is effective for many practical applications in communications area.

References

1. Steele R (1992) Mobile radio communications. Pentech, London
2. Lee WCY (1990) Mobile cellular communication systems. McGraw-Hill, New York
3. Lee WCY (1982) Mobile communication engineering. McGraw-Hill, New York
4. Fujimoto K, James JR (1994) Mobile antenna systems handbook. Artech House, Boston
5. Balanis CA (1997) Antenna theory, analysis and design, 2nd edn. Wiley, New York
6. Pozar DM (1998) Microwave engineering, 2nd edn. Wiley, USA
7. Collin RE (1992) Foundations for microwave engineering, 2nd edn. McGraw-Hill, Singapore
8. Guy RFE (1988) General radiation-pattern synthesis technique for array antennas of arbitrary configuration and element type. IEEE Proc H Microw Anten Propagat 135(4):241–248
9. McEwan NJ, Ibrahim BAW, Sadeghzadeh RA, Abdulmula EA, Qassim KAS (1995) Pattern shaping for handset antennas. In: 9th international conference on antennas and propagation, vol 1, pp 106–110
10. Mitchell RJ, Chambers B, Anderson AP (1996) Array pattern synthesis in the complex plane optimised by a genetic algorithm. Electron Lett 32(20):1843–1845
11. Saka B, Yazgan E (1997) Pattern optimization of a reflector antenna with planar-array feeds and cluster feeds. IEEE Trans Anten Propagat 45(1):93–97
12. Zhou PY, Ingram MA (1998) A new synthesis algorithm with application to adaptive beamforming. In: 9th IEEE SP workshop on statistical signal and array processing, pp 21–24
13. Dotlic I, Zejak A (2001) Pattern side lobe level suppression on antenna array with arbitrary geometry by the IRLS algorithm. In: EUROCON 2001, international conference on trends in communications, vol 1, pp 167–177
14. Degli-Esposti V, Riva G, Binucci N (2003) Derivation of antenna pattern shaping criteria for urban base stations using ray tracing. IEEE Trans Veh Technol 52(6):1686–1688
15. Barba M, Page JE, Encinar JA, Montejo JR (2005) Elevation radiation pattern shaping and control in broadband base station antenna arrays. In: ICECom 18th international conference on applied electromagnetics and communications, pp 1–3
16. Moore J, Pizer R (1984) Moment methods in electromagnetics, techniques and applications. Research Studies, London
17. Hansen RC (1990) Moment methods in antennas and scattering. Artech House, Norwood, MA
18. Kraus JD (1988) Antennas, 2nd edn. McGraw-Hill, New York
19. Kennedy J, Eberhart RC (1995) Particle swarm optimization. In: IEEE conference on neural networks, vol 4, pp 1942–1948
20. Shi Y, Eberhart RC (1998) Parameter selection in particle swarm optimization. In: 7th annual conference on evolutionary programming, pp 591–600
21. Shi Y, Eberhart RC (1999) Empirical study of particle swarm optimization. In: IEEE congress on evolutionary computation, vol 3, pp 1945–1950
22. Eberhart RC, Shi Y (2001) Particle swarm optimization—developments, applications and resources. In: IEEE congress on evolutionary computation, vol 1, pp 81–86
23. Clerc M, Kennedy J (2002) The particle swarm—explosion, stability, and convergence in a multidimensional complex space. IEEE Trans Evol Comput 6(1):58–73
24. Shi Y, Eberhart RC (1998) A modified particle swarm optimizer. In: IEEE congress on evolutionary computation, pp 69–73
25. Kennedy J (1999) Small worlds and mega-minds—effects of neighborhood topology on particle swarm performance. In: IEEE congress on evolutionary computation, vol 3, pp 1931–1938
26. Kennedy J (2000) Stereotyping: improving particle swarm performance with cluster analysis. In: IEEE congress on evolutionary computation, vol 2, pp 1507–1512
27. Kennedy J, Eberhart RC, Shi Y (2001) Swarm intelligence. Morgan Kaufmann, San Francisco
28. Eberhart RC, Shi Y (2002) Comparing inertia weights and constriction factors in particle swarm optimization. In: IEEE congress on evolutionary computation, vol 1, pp 84–88
29. Gies D, Rahmat-Samii Y (2003) Particle swarm optimization for reconfigurable phase-differentiated array design. Microw Opt Technol Lett 38(3):168–175
30. Robinson J, Rahmat-Samii Y (2004) Particle swarm optimization in electromagnetics. IEEE Trans Anten Propagat 52(2):397–407
31. Lukeš Z, Raida Z (2005) Multi-objective optimization of wire antennas: genetic algorithms versus particle swarm optimization. Radioengineering 14(4):91–97
32. Xu S, Rahmat-Samii Y, Gies D (2006) Shaped-reflector antenna designs using particle swarm optimization: an example of a direct-broadcast satellite antenna. Microw Opt Technol Lett 48(7):1341–1347